Thermo-mechanical model of a cardboard-plaster-cardboard composite plate submitted to fire load and experiments

S. Sakji, Christian Soize, J.-V. Heck

Thermo-mechanical model of a cardboard-plaster-cardboard composite plate submitted to fire load and experiments

S. Sakji[1,2], C. Soize[2], J.V. Heck[1]
[1] *Modelling laboratory, CSTB Marne-La-Vallée, France.*
[2] *Mechanics laboratory, Marne-la-Vallée University, France*

Abstract

Generally, the standard rules require conventional tests at scale one in order to justify the fire resistance of loaded plasterboard-lined partitions. This paper corresponds to a project whose objectives are to develop a numerical simulation model validated with experiments in order to predict thermo-mechanical overall partition behaviour. This research is organized in four steps. The first step is to set on an experimental thermo-mechanical data base for multilayer cardboard-plaster-cardboard(CPC). These tests are carried out using a new testing bench specially developed for this research. A full description of this device is given in the paper. In order to prepare the implementation of a probabilistic model for the CPC multilayer, several tests are performed for different thermo-mechanical configurations. The second step of the research is the development of a complete thermo-mechanical model for CPC multi-layer plates. The developed model is adapted to a range of temperatures for which the cardboard and the plaster can be destroyed. The mathematical-mechanical model has been developed in order to simulate the thermo-mechanical behaviour of the CPC panels subjected to a heat flow corresponding to the ISO 834 function. Numerical simula-

tions performed with a dedicated finite element code are presented. The third step is the identification of the thermo-mechanical parameters for each material of the CPC plasterboard. Thermo-mechanical bending tests for plaster and thermo-mechanical tensile tests for each cardboard are performed. Results show an important dispersal of the Young modulus which will justify the implementation of a probabilistic model which is still in progress. The fourth step consists in comparing numerical results to the thermo-mechanical experiments of step one and to validate the developed model.
keywords: thermo-mechanical model, cardboard-plaster-cardboard composite plate, fire engineering, high light-framed walls

1 Introduction

Large height partitions (10 meters or more) are unload bearing structures. They are made of plasterboards screwed on both sides of a metal frame of various construction configurations. Besides structural requirements such as the resistance to impact loading and collision loads, a light partition must verify various fire resistance criteria. Fire resistance requirements specify the carrying out of full scale tests under the ISO834 thermal loading curve. This last requirement cannot be met when the structure dimensions exceed those of the testing furnaces (up to 5 m). One popular way to circumvent this dimensional difficulty consists in evaluating the partition behaviour by means of an experimental and numerical combined approach. Benouis [1] adopted this approach to assess the mechanical behaviour of light partitions at room temperature. Plasterboard, a cardboard-plaster-cardboard (CPC) multilayer, gives a partition higher resistance under fire loading thanks to the important quantity of capillary and chemically bound water contained in the plaster(21% of its weight). The first step of this research deals with studying the CPC mechanical characteristics under fire and mechanical loading. For that one adopts a thermo-mechanical approach taking implicitly the hydrous phase into account. Indeed the mechanical characteristics of the CPC multilayer are determined under the same thermal loading that a partition would receive during conventional resistance test. For this matter a new thermal loading bench (TLB) is designed allowing a thermal load history equivalent to the ISO834 function to be reproduced on CPC and then to perform mechanical tests. In accordance with the experimental protocol described, other thermo-mechanical tests were performed on cardboard and plaster. A thermo-mechanical model following the classical one-dimensional homogenization theory has been developed. In the model, one introduces a cut-off damage variable for each layer of the CPC. A devoted finite elements code, taking into account the evolution of damage within the layers, has been developed. The numerical simulation results are then compared to experimental ones.

2 Methods

2.1 Experimental identification of the thermo-mechanical behaviour of CPC

To identify the mechanical characteristics of CPC submitted to a thermal load, a thermo-mechanical approach taking into account the hydrous phase is adopted. Actually, the experimental approach is developed in two steps:

1. Thermal loading by means of a thermal load bench (TLB) specially conceived for this work
2. Mechanical characterization by means of a four point bending test.

2.1.1 Thermal load bench

The TLB (fig.1) allows us to reproduce on $0.4 \times 0.4\,m^2$ specimens an incidental flux equivalent to the one that a partition would receive during a mandatory test using a gas furnace. It is composed of a radiant panel which is the heat radiant source and of a mobile cart provided with a specimen holder. The heat flux received by the specimen is modified by moving it with respect to the radiant panel. The specimen is placed on the mobile cart which is moved step by step by an engine. Hence, one can reproduce the ISO thermal load equivalent heat flux not by modifying the flow of combustible gas, as during tests in conventional furnaces, but by modifying the distance between the specimen and the radiant panel.

The plasterboard thermal loading takes place only when the radiant panel has reached its steady state. Therefore one can consider the illumination as constant throughout a test duration. The combination of a heat source used in its steady state and a specimen movement controlled with a millimeter precision insures an excellent reproducibility of the thermal load. However the ECHAFO software [2] developed in order to model thermal exchanges in fire resistance furnaces, allowed the exact calculation of the total heat flux received by the specimen surface at different time steps of conventional fire resistance test. At first, one characterized the incident heat flux received by a fluxmeter at different distances from the radiant panel, one then determined then the cart displacement program in order to reproduce by the TLB the incidental heat flux calculated by ECHAFO. The curve plotted in fig.2 shows

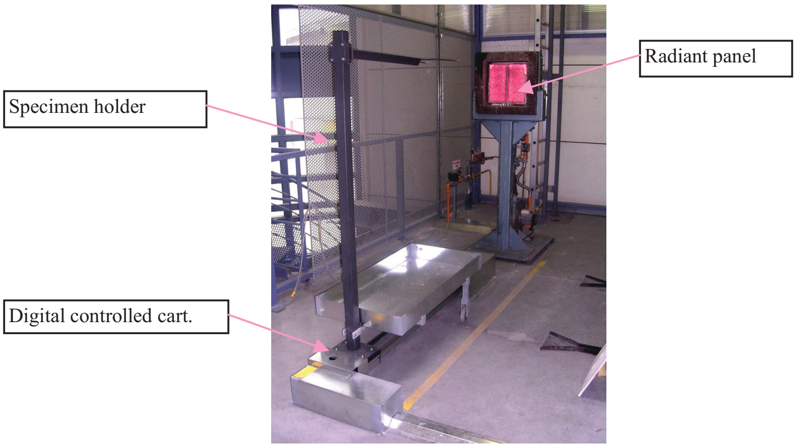

Figure 1: Thermal load bench.

Echafo total calculated incidental heat flux on the surface of a plasterboard specimen submitted to the ISO temperature load in a conventional furnace and the TLB proposed heat flux.

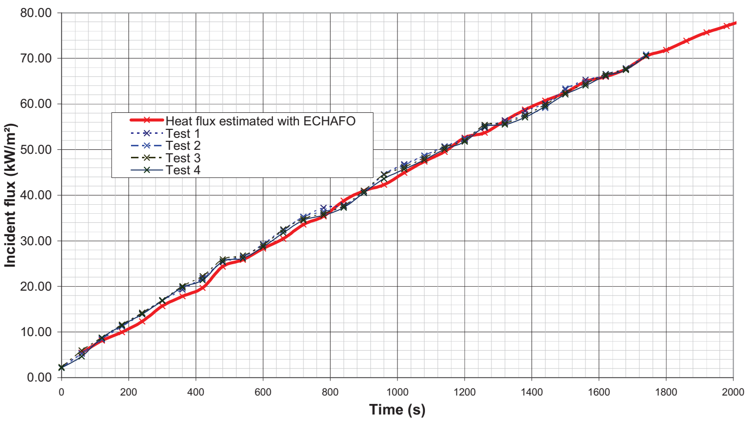

Figure 2: Graphs of the measured heat flux (vertical axis in kW/m^2) as a function of time (horizontal axis in s): ECHAFO estimated heat flux (solid line), TLB measured heat flux (test1,2,3,4).

2.1.2 Mechanical load bench

The second step of the experimental protocol concerns mechanical characterization tests of the CPC multilayer and its components. The Young modulus of CPC multilayer corresponding to different time steps of the ISO thermal load has been determined. Therefore, after having exposed a $0.4 \times 0.4\, m^2$ specimen to a historic of heat flux using the TLB, one cuts an $0.08 \times 0.4\, m^2$ specimen in the initial specimen central part. A four point bending test is then performed less than 30 seconds after the TLB specimen heat loading. The choice of the specimen dimensions (cutting out a $0.08 \times 0.4\, m^2$ specimen in the initial specimen) is motivated by the concern of preserving the hydrous boundary conditions by avoiding the steam loss in the specimen central part. Concerning cardboard characterization the same protocol is adopted and instead of the bending test, tensile tests are performed. These mechanical tests are achieved using an INSTRON press of 500 daN capacity and a $5.10^{-3} m/minute$ displacement rate.

2.1.3 Thermo-mechanical experimental results

To identify the thermo-mechanical characteristics of a BA13 STD plasterboard, tests on specimens having the geometrical characteristics described above, are performed. As the plasterboard is an orthotropic material, the bending tests were carried out in the longitudinal (LL), transversal (TT) and diagonal (LT) directions at different steps of the ISO thermal loading (ambient temperature, 300s ISO, 420s ISO and 600s ISO). For every configuration (mechanical load direction / thermal load historic) six specimens were tested. The mean value of these six tests is shown in fig. 5. During these bending tests the fire exposed face of the specimen is in tension. A measure of temperature using a thermocouple located in the middle of the plasterboard gave a correspondance between the ISO loading time and the average temperature of the plasterboard.

2.1.3.1 Comments Tests on CPC shows a non-linear behaviour which is greater at room temperature. As the exposition time increases the CPC behaviour becomes linear. Tests also show an important dispersal with regards to maximum admissible stress and Young's modulus. This dispersal result is probably due to the geometrical non-regularity of CPC plates.

2.2 CPC multilayer model

Let us consider a CPC multilayer where the plaster is modelled by n layers. The classical one-dimensional homogenization through the thickness of the

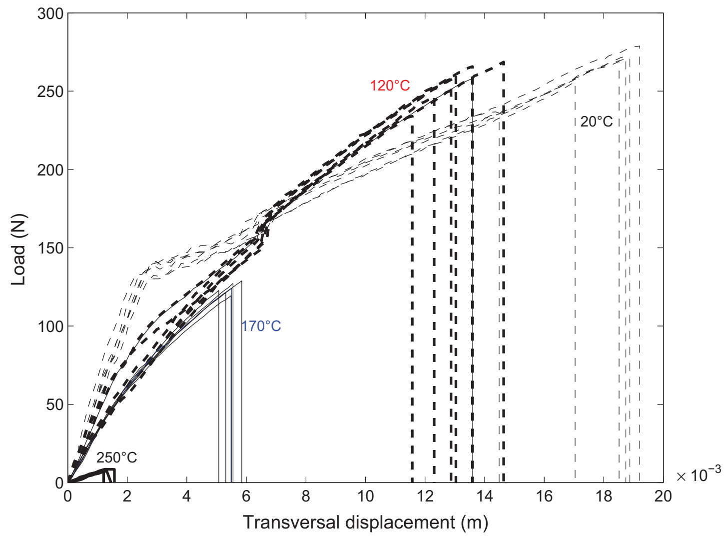

Figure 3: Experiments for different values of temperature on CPC specimens: Graphs of the mechanical load (vertical axis in N) as a function of the transversal displacement (horizontal axis in meters): Thick solid line (250°C), thin solid line (170°C), thick dashed line (120°C), thin dashed line (20°C).

multilayer (see [3], [4]) gives the relationship between global forces as a function of the global deformations and can be written by

$$\begin{pmatrix} \mathfrak{n}_1 \\ \mathfrak{n}_2 \\ \mathfrak{n}_6 \\ - \\ \mathfrak{m}_1 \\ \mathfrak{m}_2 \\ \mathfrak{m}_6 \\ - \\ \mathfrak{n}_4 \\ \mathfrak{n}_5 \end{pmatrix} = \begin{pmatrix} \underline{H}_{11} & \underline{H}_{12} & \underline{H}_{16} & | & \underline{B}_{11} & \underline{B}_{12} & \underline{B}_{16} & | & 0 & 0 \\ \underline{H}_{12} & \underline{H}_{22} & \underline{H}_{26} & | & \underline{B}_{12} & \underline{B}_{22} & \underline{B}_{26} & | & 0 & 0 \\ \underline{H}_{16} & \underline{H}_{26} & \underline{H}_{66} & | & \underline{B}_{16} & \underline{B}_{26} & \underline{B}_{66} & | & 0 & 0 \\ -- & -- & -- & -- & -- & -- & -- & -- & -- & -- \\ \underline{B}_{11} & \underline{B}_{12} & \underline{B}_{16} & | & \underline{C}_{11} & \underline{C}_{12} & \underline{C}_{16} & | & 0 & 0 \\ \underline{B}_{12} & \underline{B}_{22} & \underline{B}_{26} & | & \underline{C}_{12} & \underline{C}_{22} & \underline{C}_{26} & | & 0 & 0 \\ \underline{B}_{16} & \underline{B}_{26} & \underline{B}_{66} & | & \underline{C}_{16} & \underline{C}_{26} & \underline{C}_{66} & | & 0 & 0 \\ -- & -- & -- & -- & -- & -- & -- & -- & -- & -- \\ 0 & 0 & 0 & | & 0 & 0 & 0 & | & \underline{F}_{44} & \underline{F}_{45} \\ 0 & 0 & 0 & | & 0 & 0 & 0 & | & \underline{F}_{45} & \underline{F}_{55} \end{pmatrix} \begin{pmatrix} e_1^m \\ e_2^m \\ e_6^m \\ - \\ \kappa_1 \\ \kappa_2 \\ \kappa_6 \\ - \\ e_4 \\ e_5 \end{pmatrix} - \begin{pmatrix} h_1' \\ h_2' \\ h_6' \\ - \\ b_1' \\ b_2' \\ b_6' \\ - \\ 0 \\ 0 \end{pmatrix} \Delta T \tag{1}$$

where $h_i' = \underline{H}_{ij}\alpha_j, (i,j = 1,2,6)$, $b_i' = \underline{B}_{ij}\alpha_j, (i,j = 1,2,6)$. The terms $\underline{H}_{ij} = \sum_{k=1}^{n+2} \underline{\widetilde{Q}}_{ij}^{k}(\mathbf{x})(z_k - z_{k-1})$ correspond to the stiffness relating the global membrane forces n_i to membrane deformation $e_i^m, (i,j = 1,2,6)$.

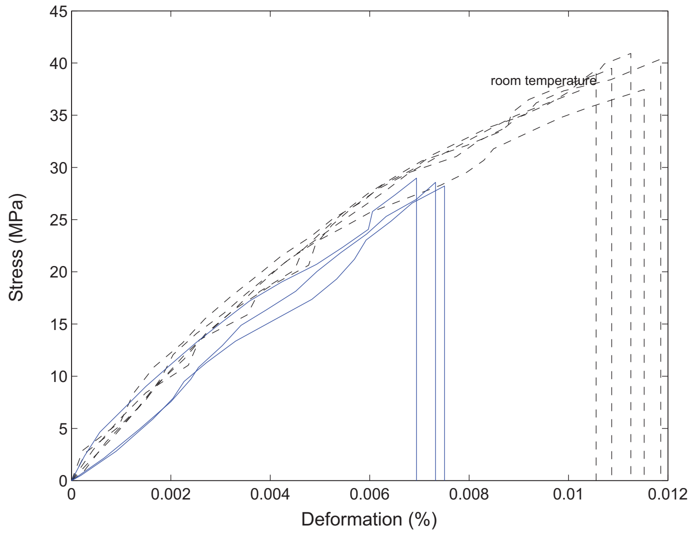

Figure 4: Experiments for different values of temperature on cardboard specimens: Graphs of the mechanical stress (vertical axis in MPa) as a function of longitudinal deformation (horizontal axis in %) :Solid lines (after 300s of TLB thermal load), dashed lines (at ambient temperature).

The terms $\underline{C}_{ij} = \underline{C}_{ji} = \frac{1}{3}\sum_{k=1}^{n+2} \underline{\widetilde{Q}}_{ij}^{k}(\mathbf{x})(z_k^3 - z_{k-1}^3), (i,j = 1,2,6)$ correspond to the global bending stiffness relating the global bending moments m_i to the global bending deformations $\kappa_i, (i = 1,2,6)$. The terms $\underline{B}_{ij} = \underline{B}_{ji} = \frac{1}{2}\sum_{k=1}^{n+2} \underline{\widetilde{Q}}_{ij}^{k}(\mathbf{x})(z_k^2 - z_{k-1}^2), (i,j = 1,2,6)$ correspond to the bending-membrane coupling terms. The terms $\underline{F}_{ij} = \underline{F}_{ji} = \varsigma_{\underline{ij}}\sum_{k=1}^{n+2} \underline{\widetilde{Q}}_{ij}^{k}(\mathbf{x})(z_k - z_{k-1}), (i,j = 4,5)$ correspond to the shear plate stiffness in which $\varsigma_{\underline{ij}}$ is the transversal shear stress correcting factor. One has $\underline{\widetilde{Q}}_{ij}^{k}(\mathbf{x}) = (1-\underline{d}_{ij}^{k}(\mathbf{x}))\underline{Q}_{ij}^{k}(\mathbf{x})$ in which $\underline{Q}_{ij}^{k}(\mathbf{x})$ and $\underline{d}_{ij}^{k}(\mathbf{x})$ are respectively the membrane stiffness and the damage parameter of the layer k. Finally one has $\underline{Q}_{11}^{k} = \frac{E_1^k}{1-\nu_{21}^k\nu_{12}^k}$, $\underline{Q}_{12}^{k} = \frac{\nu_{21}^k E_1^k}{1-\nu_{21}^k\nu_{12}^k}$, $\underline{Q}_{21}^{k} = \frac{\nu_{21}^k E_2^k}{1-\nu_{21}^k\nu_{12}^k}$, $\underline{Q}_{22}^{k} = \frac{E_2^k}{1-\nu_{21}^k\nu_{12}^k}$, $\underline{Q}_{66}^{k} = G_{13}^k$ et $\underline{Q}_{61}^{k} = \underline{Q}_{16}^{k} = \underline{Q}_{26}^{k} = \underline{Q}_{62}^{k} = 0$.

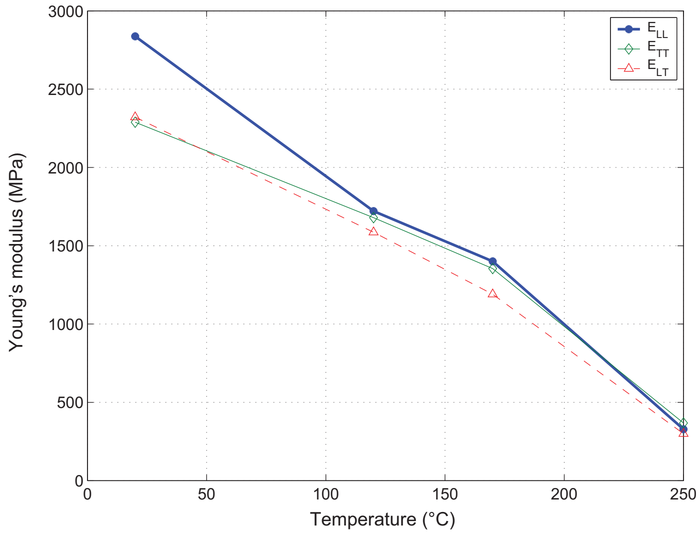

Figure 5: Experiments on CPC for different directions: Graph of the mean Young's modulus (vertical axis in MPa) as a function of the average temperature of the CPC (horizontal axis in C): Thick solid line (E_{LL}), thin solid line (E_{TT}), dashed line (E_{LT}).

2.2.1 Numerical model

A multilayer thin plate theory is used with the constitutive equation defined by eqn. (1) for the non-linear thermo-elastic model. A finite element code using 8-nodes multilayer plate elements has been developed. In a first step the temperature field is calculated. In a second step, the mechanical response is calculated as a function of the external load and the temperature. For each point of the material, the damage is zero if the maximum stress is less than the limit stress and equal to 1 if the maximum stress is equal or greater than the limit stress. It should be noted that there is one damage coefficient for each layer of each element of the discretized domain.

2.2.2 Model results

Figures 6.a and 5.b enable to compare the experiment results to the numerical simulation for the applied mechanical load as a function of the transversal displacement at 20°C (fig. 6.a) and at 120°C (fig. 6.b). Figure 6.b shows a good agreement. It should be noted some differences in figure 6.a for the ambient temperature (20°C) which are probably due to the simplified damage model used.

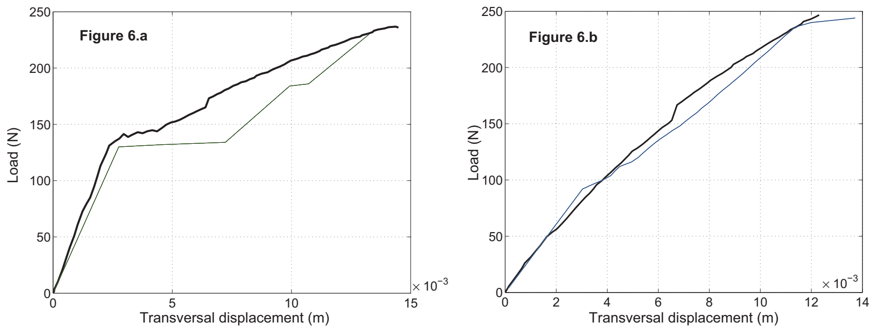

Figure 6: Mechanical applied load (vertical axis in N) as a function of the transversal displacement (horizontal axis in meters): Experiments (thick solid line), numerical simulation (thin solid line). Figure 6.a: tests at 20°C, figure 6.b: tests after 300s of thermal load

3 Conclusion

A thermal bench test has been specially developed for this work. It enabled us to perform the mechanical characterization of plasterboards submitted to the same thermal history that a light partition would receive during a conventional fire resistance test. The simulation results of the developed multilayer model show a good qualitative agreement with the experiments. In order to improve the prediction of the non-linear multilayer thermo-elastic model a more sophisticated damage model should be developed. The development of a probabilistic model of uncertainties is also in progress.

References

[1] A. Benouis. *Comportement mécanique des ouvrages en plaque de plâtre sur ossature métallique*. PhD thesis, Ecole nationale des ponts et chaussées, septembre 1995.

[2] M. Curtat Ph. Fromy. Heat transfer in fire resistance furnaces piloted with thermocouples or plate thermometers. *fire safety science -proceeding of the six international symposium*, pages 531–542.

[3] M.H. Philippe. *Etude de quelques modélisations de structures en composite a haute rigidité en flexion*. PhD thesis, Ecole nationale des ponts et chaussées, avril 1997.

[4] C. Decolon. *Structures composites, calcul des plaques et poutres multicouches*. Hermes, 2000.